Journal of Materials Chemistry A

Preparation of Brookite Titania Quasi Nanocubes and Their Application in Dye-Sensitized Solar Cells

Journal:	*Journal of Materials Chemistry A*
Manuscript ID:	TA-ART-12-2014-006746.R1
Article Type:	Paper
Date Submitted by the Author:	05-Feb-2015
Complete List of Authors:	Xu, Jinlei; Wuhan University, Department of Chemistry; Wuhan University, Chemistry Li, Kan; Wuhan University, Department of Chemistry Wu, Shufang; Wuhan University, Department of Chemistry Shi, Wenye; Wuhan University, Department of Chemistry Peng, Tianyou; Wuhan University, Department of Chemistry

Journal Name

RSCPublishing

ARTICLE

Preparation of Brookite Titania Quasi Nanocubes and Their Application in Dye-Sensitized Solar Cells

Cite this: DOI: 10.1039/x0xx00000x

Jinlei Xu, Kan Li, Shufang Wu, Wenye Shi, and Tianyou Peng*

Received 00th January 2014,
Accepted 00th January 2014

DOI: 10.1039/x0xx00000x

www.rsc.org/MaterialsA

Brookite TiO_2 quasi nanocubes with high phase purity and thermal stability are synthesized through a hydrothermal process. The obtained brookite TiO_2 quasi nanocubes have a mean size of ~50 nm with a specific surface area of ~34.2 m^2 g^{-1}. By using as photoanode material, the single brookite TiO_2 nanocubes film-based dye-sensitized solar cell (DSSCs) shows a higher open-circuit voltage but lower conversion efficiency than the single nanosized anatase TiO_2 film-based one with a similar film thickness; while using the brookite TiO_2 nanocubes as overlayer of the nanosized anatase TiO_2 film, the fabricated bilayer solar cells exhibit significant enhancement in both the open-circuit voltage and short-circuit current, and the corresponding bilayer solar cell with an optimized overlayer thickness gives a conversion efficiency up to 8.83%, with 23.8% improvement as compared to the single anatase cell (7.13%). The brookite nanocubes as overlayer not only reduce the charge recombination and dark current, but also prolong the electron lifetime, which leads to the enhanced voltage and photocurrent, and then the improved photovoltaic performance of the bilayer solar cell. These results demonstrate that the simple fabrication method of the brookite TiO_2 nanocubes and their application as overlayer are promising, which offers a strategy for the development of the low-cost and high efficiency DSSCs through tuning the photoanode's component and structure.

***Keywords*:** Brookite titania nanocube; bilayer TiO_2 film; dye-sensitized solar cell; conversion efficiency; photoelectrochemical property

1 Introduction

Among the three crystallographic forms of titania (TiO_2) existing in nature, only anatase, rutile and/or their mixed crystal have been widely studied and applied in the fields of photocatalysis[1,2] and dye-sensitized solar cells (DSSCs).[3,4] Nevertheless, brookite TiO_2 has the highest bandgap energy (E_g) among the three TiO_2 polymorphs,[5,6] which can contribute the most negative conduction band (CB) level because the three crystal phases have similar valence band (VB) level due to the same elementary composition.[5-7] This readily suggests that brookite TiO_2 should exhibit a higher open-circuit voltage (V_{OC}) for the DSSCs[8] and a better photocatalytic activity[9] than anatase and rutile. However, there are few reports on the brookite's photocatalytic[9] and photovolatic[10-14] applications up till now, although it is reported that brookite TiO_2 has a higher photoactivity than rutile and anatase TiO_2 as early as 1985.[7] The first DSSC using a mixture containing 75% brookite and 25% anatase as the semiconducting electrode is reported in 2002,[10] and it was found that the short-circuit photocurrent density (J_{SC}) increased approximately linearly to the film thickness but with slight decreases in the open-circuit voltage (V_{OC}) and fill factor (FF) values.[10] Thus, the resulted solar cell fabricated with 5 μm thick mixed phase TiO_2 film showed an efficiency of 4.1%, comparable to the results obtained in anatase films with a similar thickness.[10] Thereafter, some single brookite film-based solar cells have been fabricated,[11-15] and a record efficiency of the single brookite solar cells is ~5.97%.[12,13] Nevertheless, those brookite solar cells showed higher V_{OC} than the anatase ones,[11-15] implying brookite is also a promising electrode material of DSSCs.

One difficulty for the brookite's photovoltaic applications is the preparation of brookite TiO_2 with high phase purity due to its thermodynamic instability, and the majority of attempts for the pure phase brookite TiO_2 only obtained mixed crystal containing brookite particles with a secondary phase such as anatase and/or rutile.[16-20] For example, Kandiel and co-workers[16] have found that the brookite/anatase ratio can be tuned *via* changing the urea concentration by using titanium bis(ammoniumlactate) dihydroxide as Ti source, but a pure brookite was still difficult to obtain. Similarly, TiO_2 nanorods containing anatase/rutile/brookite mixed crystal were synthesized by using tetrabutyl-titanate as raw material in an

College of Chemistry and Molecular Science, Wuhan University, Wuhan 430072, P. R. China. E-mail: typeng@whu.edu.cn; Tel. & fax: +86-27 6875 2237.

acidic condition.[17] In 2007, Li and coworkers[18] found that enhancing the solution pH from 1.32 of a fixed $TiCl_3$ concentration (62.5 mM) causes the cocrystallization of anatase, steadily decreasing the brookite content and finally leading to pure anatase at pH >9.0, while decreasing the pH leads to the co-formation of rutile and eventually pure rutile at pH 0.44 or below.[18] Under the same solution pH (1.32) but varying the initial $TiCl_3$ concentration, pure brookite tends to form under intermediate $TiCl_3$ concentration, and either increasing or lowering the concentration yielded more anatase in the final product.[18] Moreover, Mitsuhashi and Watanabe[19] found that the brookite was crystallized by hydrothermal treatment at 220-560°C of the precipitate prepared from $TiCl_4$ and $CaCl_2$ solution. Arnal and coworkers[20] also found that brookite was formed together with rutile by sol-gel reaction of $TiCl_4$ and tert-butyl alcohol at 110°C. It is understandable that high-quality brookite has seldom been obtained sine it is a metastable phase with a relatively low symmetric structure.[21-26]

Until 2009, high-quality brookite TiO_2 with high phase purity was synthesized by optimizing the Na^+ and OH^- concentrations in a reaction system, and the obtained flower-like brookite showed a direct transition with a bandgap energy (E_g) of 3.4 eV,[21] which is obviously larger than those of the other polymorphs, that is, an indirect bandgap of 3.2 eV for anatase and a direct bandgap of 3.0 eV for rutile.[21] Thereafter, brookite nanosheets with specific facets exposed, which turned catalysts from inert to high photoreactivity, were also synthesized by a similar process.[27] Although the E_g of the above flower-like brookite was estimated to be 3.4 eV according to the plot of $(F(R)* hv)^n$ versus energy (hv), which is almost the same as that (3.4 eV) of the brookite nanoparticles reported by Koelsch et al,[22] the E_g of brookite is unsettled and more variations exist in the literatures.[18,23,24] For example, Li and coworkers[18] found that both the optical bandgap (3.11 eV) and the indirect bandgap (2.85 eV) of brookite lie in between those of anatase and rutile, while Zallen and Moret[23] thought that the lowest direct bandgap for brookite is larger than 3.54 eV. Moreover, a brookite E_g of 3.14 eV was also reported by Grätzel and Rotzinger.[24] The above phenomena indicated that the E_g of brookite might depend upon the product source, morphology and particle size, which need further investigation.

Recently, thermally stable brookite TiO_2 with single phase and rice-like morphology was prepared through a hydrothermal method by using $Ti(SO_4)_2$ as Ti source and NaOH solution as the regulating agent in our group,[28] and its average diameter (brachyaxis of the rice-like particle) can be widely tuned in the range of 200-1200 nm by varying the reaction condition, and those rice-like brookite TiO_2 particles with high phase purity and ~600 nm particle diameter as overlayer can noticeably improve the photovoltaic performance of the anatase-based solar cells.[28,29] Herein, thermally stable brookite TiO_2 nanocubes with high phase purity and much smaller sizes (~50 nm) are successfully synthesized through a hydrothermal method by using $TiCl_4$ as Ti source. By using as photoanode material, the single brookite TiO_2 solar cell shows a higher open-circuit voltage but lower conversion efficiency than the anatase cell with a similar film thickness, which is fabricated with a commercial nanosized anatase TiO_2 (particle size of ~20 nm) paste. Moreover, by using the brookite TiO_2 nanocubes as overlayer of the nanosized anatase TiO_2 film, the fabricated bilayer solar cell can achieve efficiency up to 8.83%, improved by 23.8% as compared to the single anatase cell (7.13%). The functioning of the brookite TiO_2 overlayer on the anatase film was investigated by using spectroscopic, electrochemical and photoelectrochemical measurement techniques.

2 Experimental section

2.1 Material preparation

All reagents are of analytical grade and used as received without further purification. A typical preparation process of brookite TiO_2 nanocubes is as follows: A fixed amount of $TiCl_4$ was added drop by drop to a Teflon autoclave containing 40 mL deionized water cooled by an ice-water bath, and then 2.0 g urea was mixed and dissolved in this solution with agitation. After that, 2.0 mL of sodium lactate liquor (60%) was dropped in the mixed solution while stirring for 30 min. The clarified liquid obtained was then subjected to hydrothermal treatment at 200°C for 20 h. After that, the white precipitate was separated by centrifugation (4000 rpm), and then washed several times with distilled water and absolute ethanol, dried at 70°C in air. Finally, the as-prepared product was further calcined at 500°C for 3 h with a heating rate of 2°C min^{-1}.

2.2 Material characterization

Phase analyses with X-ray diffraction (XRD) method were performed on a D8-advance X-ray diffractometer (Bruker) with CuKα radiation (λ=0.15418 nm). A scan rate of 2° min^{-1} was applied to record the XRD patterns in the range of $20^o \leq 2\theta \leq 50^o$. The microstructures were explored by a high-resolution transmission electron microscope (HRTEM; JEM 2100F). The morphology was investigated by scanning electron microscope (SEM; JSM-6700F). Nitrogen adsorption-desorption isotherms at 77 K were measured on a Micrometrics ASAP 2010 system after samples were degassed at 120°C. UV-vis diffuse reflectance absorption spectra (DRS) were obtained with a Shimadzu UV-3600 UV-vis-NIR spectrophotometer equipped with an integrating sphere with $BaSO_4$ as the reference. Raman spectra were obtained on confocal UV-vis Raman spectrometer (Renishaw, RM-1000) with an excitation line of 514.5 nm.

2.3 Photoanode preparation and solar cell fabrication

Typically, brookite TiO_2 paste is prepared as follows: A 1.0 g portion of the brookite TiO_2 nanoparticles were mixed with 5.0 mL of ethanol, 0.2 mL of aceticacid, 3.0 g of terpinol and 0.5 g of ethyl cellulose by ball-milling for 10 h with agate beads as media. TPP3 paste containing anatase TiO_2 nanoparticles with particle size of ~20 nm was obtained from Hep-tachroma Co, Ltd. Brookite TiO_2 electrode is prepared by spreading the brookite TiO_2 paste on a clean FTO glass (15 Ω sq^{-1}) by using the doctor blading technique. Film thicknesses was controlled

by adhesive tape (Scotch, 50 μm) serving as spacer. After drying in atmosphere, the film was sintered at 500°C for 30 min. Similarly, the nanosized anatase TiO_2 electrode is prepared by using TPP3 paste as mentioned above. If necessary, the brookite TiO_2 paste is further spread on the above nanosized anatase TiO_2 film, and then sintered at 500°C for 30 min again to remove the binders to obtain the bilayer photoanode.

Dye sensitization was achieved by soaking the film electrode into a 0.3 mM N719 (Solaronix) ethanol solution for 20 h, followed by rinsing in ethanol and drying in air. The dye-sensitized electrode was assembled in a typical sandwich-type cell. A Pt-coated FTO counter electrode was placed over the dye-sensitized electrode. The electrolyte which consists of 0.5 M LiI, 0.05 M I_2 and 0.1 M 4-tert-butylpyridine in 1:1 acetonitrile-propylene carbonate was injected into the interspaces between the electrodes to fabricate the solar cell.

2.4 Solar cell performance measurement

The solar cell was illuminated by light with energy of 100 mW cm^{-2} (AM1.5G) from a 300 W solar simulator (Newport, 91160). The light intensity was determined using a reference monocrystal silicon cell (Oriel, U.S.). Computer-controlled Keithley 2400 sourcemeter was employed to collect the photocurrent-voltage (J-V) curves of DSSCs. The active area was 0.16 cm^2. To estimate the dye-adsorbed amount of TiO_2 films, the sensitized electrode was separately immersed into a 0.1 M NaOH solution in a mixed solvent (V_{water}: $V_{ethanol}$=1:1), which resulted in the desorption of N719. The absorbance of the resulting solution was measured by a UV-3600 UV-vis spectrophotometer (Shimadzu, Japan). The dye-adsorbed amount was determined by the molar extinction coefficient of 1.41×10^4 dm^3 mol^{-1} cm^{-1} at 515 nm as reported previously.[30]

The incident photon-to-current conversion efficiency (IPCE) was measured as a function of wavelength from 250 to 850 nm by using a Model QE/IPCE system (PV Measurements Inc.). Electrochemical impedance spectroscopy (EIS) was obtained by applying bias of the open-circuit voltage without electric current under 100 mW cm^{-2} illumination and were recorded over a frequency range of 0.05-10^5 Hz with ac amplitude of 10 mV. For the photoinduced open-circuit voltage decay (OCVD) measurements, the illumination was turned off using a shutter after the cell was first illuminated to a steady voltage, and then the OCVD curve was recorded. The above measurements were carried out on a CHI-604C electrochemical analyzer.

3 Results and discussion

3.1 Crystal phase and microstructure analyses

Fig. 1 depicts the XRD patterns of the as-synthesized brookite TiO_2 and its calcined product at 500°C. Both of the products are orthorhombic brookite TiO_2 (JCPDS 65-2448), and the diffraction peaks at 2θ = 25.3°, 25.7°, 30.8°, 36.2°, 37.3°, 40.1°, 42.4°, 46.0°, 48.0°, and 49.1° are ascribable to the reflection of (210), (111), (211), (102), (021), (202), (221), (302), (321), and (312) plane of the brookite TiO_2,[9,21,27,28] respectively. Clear and

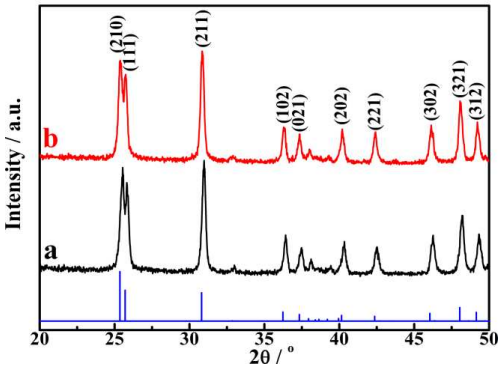

Fig. 1 XRD patterns of the as-synthesized brookite TiO_2 (a), and its calcined product at 500°C (b)

sharp diffraction peaks of brookite without any other crystal phase indicate that those products have high crystallinity and phase purity.[9,21] After heat treatment at 500°C, only diffraction peaks of brookite that become slightly stronger and sharper are identified in Fig. 1b. The average crystal sizes calculated from the broadening of the (211) peaks by using Scherrer formula are 45.3 and 50.2 nm for the products as-synthesized and calcined at 500°C, respectively. It is well known that brookite is a thermodynamic metastable phase, but the calcined product keeps all diffraction peaks of brookite, indicating the brookite TiO_2 has a relatively good thermal stability.[13,14,27-29]

Numerous studies have been proved that the anatase-to-rutile phase transformation is reconstructive and proceeds directly without involvement of the other metastable phase, but fewer investigations on the brookite phase transformation were reported,[31-33] most likely due to the difficulty to obtain high-quality pure brookite because brookite is a metastable phase with more complicated and lower symmetric structure as menioned above. Furthermore, the brookite phase formation is always accompanied by secondary phases such as anatase or/and rutile since anatase shows a relatively lower surface energy in comparison with brookite.[24] Nevertheless, those investigations on the single brookite indicated that this metastable TiO_2 polymorphs transformed directly to rutile without detection of anatase as an intermediate at high temperature, especially in the range of 800–900°C.[24,31-33] The relatively good thermal stability of the present nanocubes is beneficial for the following application in DSSCs since the photoanode should suffer from calcination at 500°C to remove the binders in the paste. Therefore, the brookite TiO_2 calcined at 500°C are use to prepare the paste in order to avoid certain unexpected change during the photoanode fabrication process.

Raman spectrum can further confirm the high crystallinity and pure brookite phase of the calcined product because it is an effective approach to distinguish the brookite from anatase.[34-37] According to the space group theory, the possible 69 optical modes of brookite lattice with D_{2h} symmetry (space group: Pbca) can be expressed by the irreducible representation including $9A_{1g}$+ $9B_{1g}$+ $9B_{2g}$+ $9B_{3g}$+ $9A_{1u}$+$8B_{1u}$ + $8B_{2u}$+ $8B_{3u}$,

in which A_{1g}, B_{1g}, B_{2g}, and B_{3g} mode are Raman active.[35,38] Raman spectrum (Fig. 2) of the brookite TiO_2 calcined at 500°C

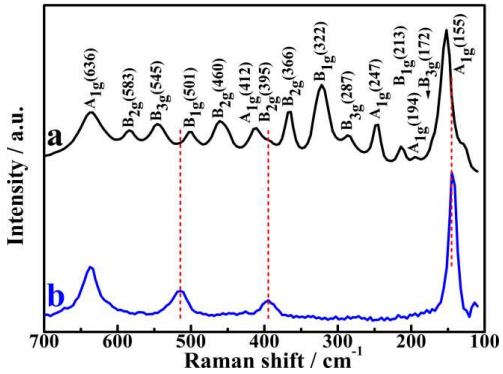

Fig. 2 Raman spectra of the calcined brookite TiO_2 (a) and anatase TiO_2 (b)

shows 15 vibration bands in the range of 100~700 cm^{-1}, which can be assigned to the modes of A_{1g} (155, 194, 247, 412, 636 cm^{-1}), B_{1g} (213, 322, 501 cm^{-1}), B_{2g} (366, 395, 460, 583 cm^{-1}), and B_{3g} (172, 287, 545 cm^{-1}) of brookite,[35] respectively. As for anatase, only six bands are reported in the same wave number range with Raman active vibration modes of A_{1g} (513 cm^{-1}), B_{1g} (399, 519 cm^{-1}), and E_g (144, 197, 639 cm^{-1}).[35] No obvious vibration bands related to the anatase especially at 513 and 397 cm^{-1} can be observed from Fig. 2, further confirming that high crystallinity and pure brookite was obtained by the present preparation processes.

Fig. 3 shows the FESEM and TEM images of the brookite TiO_2 derived from the hydrothermal reaction and calcination process. As can be seen from Fig. 3a, most of the obtained brookite TiO_2 particles have quasi nanocube-like morphology, which have relative uniform particle sizes in the range of 20-75 nm with a mean particle size of ~50 nm. Those quasi nanocubes' surfaces are relatively smooth with occasionally small irregular particles contacted on their surfaces. Meanwhile, the most of quasi nanocubes show ~90° angle between the adjacent exposed facets. The above observations can be further validated by the TEM image shown in Fig. 3b. Those quasi nanocubes show relatively smooth surfaces and sharp edges, in accordance with the observation from the above FESEM image. Those uniform perspective projections of discrete nanoparticles indicate that the nanocube-like shape is a complete particle but not an aggregate of small primary particles. Moreover, the average crystalline size (50.2 nm) calculated from the above XRD pattern is very close to the mean particle size (~50 nm), also implying the high crystallinity of those quasi nanocubes. Fig. 3c shows the HRTEM image of a single particle with much smaller size, which also shows a complete rhomb-like shape and high crystallinity, indicating those occasionally attached small particles on the nanocubes (Fig. 3a) are also a complete particle but not aggregated on the nanocube' surfaces. The HRTEM image (Fig. 3d) indicates that the lattice spacing is 0.351 nm, which is consistent with the (210) planes of brookite. The (111) lattice fringes with *d*-spacing of ~0.346 nm can be clearly observed, which corresponds to the strongest peak in the above XRD pattern. The crystal face angle of the above two crystal planes is ~79.8°, consistent with the theoretical value.[28] The clear lattice fringes reveal the single-crystal features and high crystallinity of the present brookite TiO_2 quasi nanocubes.

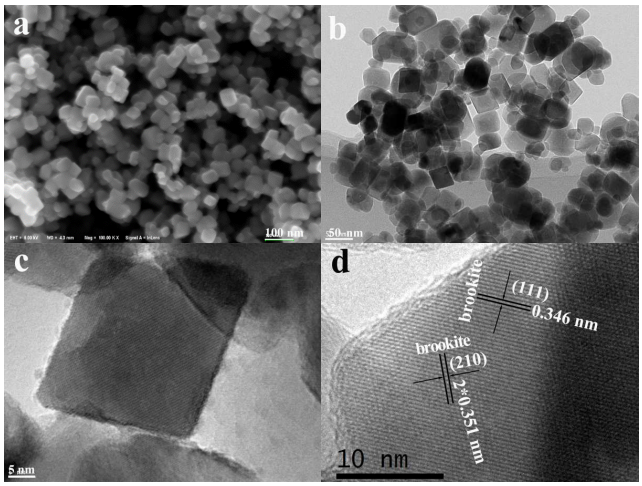

Fig. 3 FESEM (a), TEM (b) and HRTEM (c, d) images of the brookite TiO_2 nanocubes

The obtained brookite TiO_2 nanocubes shown in Fig. 4 displays a type III liquid N_2 adsorption-desorption isotherm of curve with H3 hysteresis loops, which shows a jumps in the N_2 adsorption branches starting at a very high relative pressure region (P/P_0=0.82). It can be attributed to the condensation of N_2 in the intercrystallite pores among those stacked particles. The Brunauer-Emmett-Teller (BET) specific surface area of the brookite TiO_2 nanocubes is calculated to be ~34.2 m^2 g^{-1}, slightly higher than that (~28.9 m^2 g^{-1}) of the previously reported brookite TiO_2 nanosheets with a length of ~80 nm, a width of ~60 nm and a thickness of ~15 nm,[27] but much lower than that (~175 m^2 g^{-1}) of the brookite rice-like nanoparticles with ~15 nm long and ~10 nm width.[33] The relatively low surface area of the present nanocubes is possibly due to the present preparation process. The inserted Barret-Joyner-Halenda (BJH) pore size distribution (Fig. 4) of the as-synthesized sample determined from the desorption isotherm shows a single broad distributions (10-100 nm), also attribute to the intercrystallite voids among those stacked nanoparticles.

Fig. 5 shows the UV-vis diffuse reflectance absorption spectra (DRS) of the brookite TiO_2 nanocubes and anatase TiO_2 nanoparticles with particle size of ~20 nm as the TPP3 paste. The bandgap energy of the brookite TiO_2 nanocubes and the

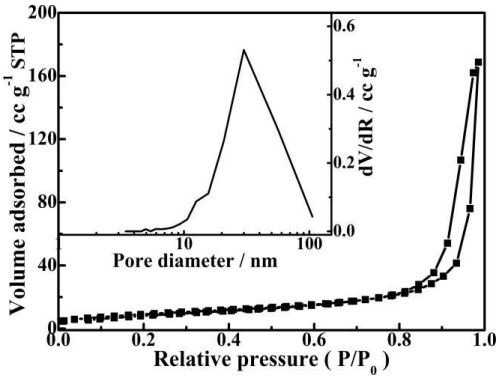

Fig. 4 Nitrogen adsorption-desorption isotherm and Barret-Joyner-Halenda (BJH) pore size distribution plots (inset) of the brookite TiO_2 nanocubes

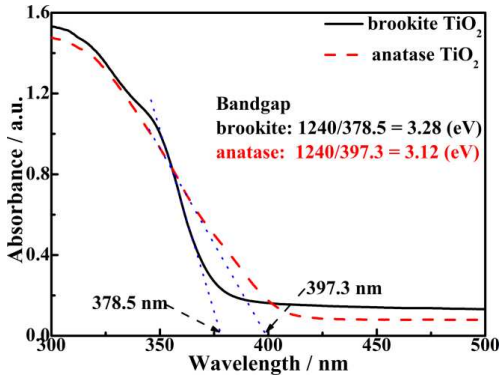

Fig. 5 UV-vis diffuse reflectance absorption spectra (DRS) of the brookite TiO_2 nanocubes and anatase TiO_2 nanoparticles with particle size of ~20 nm as the TPP3 paste

anatase TiO_2 nanoparticles can be estimated to be 3.28 and 3.12 eV according to their absorption band edges at 378.5 and 397.3 nm, respectively. The bandgap energy of the brookite TiO_2 is 0.16 eV higher than the anatase TiO_2, which is consistent with the previous investigation.[21] This two TiO_2 polymorphs should have a similar VB due to their same elementary composition,[5-7] and therefore the present brookite TiO_2 nanocubes has a higher CB or Fermi level than the anatase TiO_2 nanoparticles, which would be beneficial for enhancing the voltage of the DSSCs as shown in the following section.

3.2 Photovoltaic performance analyses of the solar cells

By using the above brookite TiO_2 nanocubes as photoanode material, the single brookite solar cells are fabricated and their current-voltage (*J-V*) curves under simulated AM1.5G illumination (100 mW cm^{-2}) were measured and shown in Fig. 6a. The corresponding short-circuit current densities (J_{SC}), open-circuit potentials (V_{OC}), fill factors (FF), and overall conversion efficiencies (η) are summarized in Table 1.

The B1 (or B2) electrode is fabricated by using the brookite TiO_2 nanocubes paste and 1 (or 2) layer of adhesive tape as spacer. As can be seen from Table 1, the B2 film-based solar cell yields a 3.92% efficiency with J_{SC}=7.38 mA cm^{-2} and V_{OC}=0.73 V, whereas the B1 film-based one shows a 2.94% efficiency with J_{SC}=6.08 mA cm^{-2} and V_{OC}=0.73 V. The obvious improvement of the photovoltaic performance of the single brookite solar cell can be attributed to the increased film thickness, which resulting in an enhanced dye loading as shown in Table 1. It means more dye excited-state electrons could be injected into TiO_2 CB, and then causing a higher photocurrent and conversion efficiency.[39] In addition, the augment of film thickness of the brookite electrode is beneficial for improving the fill factor as shown in Table 1.

In order to compare with the anatase solar cell, nanosized anatase TiO_2 film (T2 electrode) is also fabricated by using TPP3 paste and 2 layers of adhesive tape as spacer, because our previous investigation demonstrated that T2 electrode has an optimal film thickness, and its corresponding solar cell shows the highest conversion efficiency.[29] As shown in Table 1, T2 film has a thickness of ~10.6 μm, very similar to the B2 film

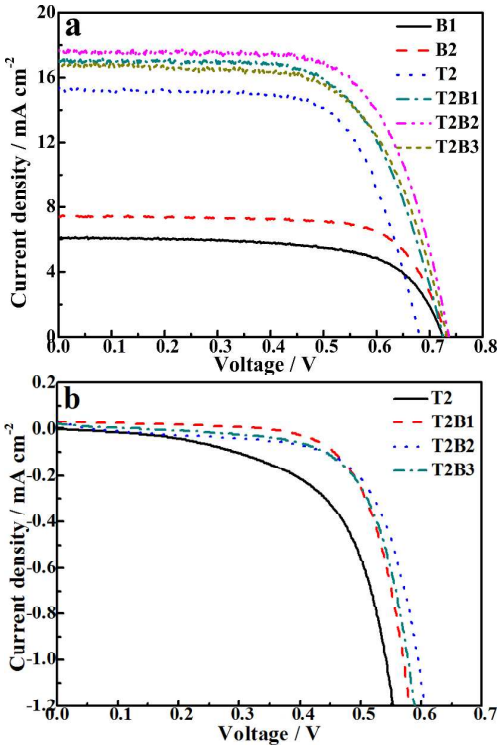

Fig. 6 Comparison of *J-V* (a) and dark current (b) curves of the DSSCs fabricated with the single brookite, anatase film and their bilayer films (T2B1,T2B2, and T2B3)

Table 1 Photovoltaic performance of the DSSCs fabricated with different electrodes

Devices	J_{SC} mA cm^{-2}	V_{OC} V	*FF*	η %	Thickness μm	Dye loading ($\times 10^{-8}$ mol cm^{-2})
B1	6.08	0.73	0.67	2.94	4.9	3.50
B2	7.38	0.73	0.72	3.92	10.8	4.94
T2	15.27	0.68	0.69	7.13	10.6	7.62
T2B1	17.04	0.72	0.66	8.10	13.9	9.43
T2B2	17.56	0.74	0.68	8.83	17.5	12.01
T2B3	16.78	0.73	0.65	8.00	20.0	12.91

(~10.8 μm), and the brookite solar cell has a V_{OC} of 0.73 V, higher than that (0.68 V) of the anatase one. This is consistent with the previous reports.[10-15] Kusumawati and co-workers have proved that the higher V_{OC} of the brookite cell than the anatase cell is due to the lower reactivity of the brookite surface, which causing a reduced charge recombination reaction.[14] In this investigations on the charge transfer reaction and charge carrier transport processes using the impedance spectroscopy (IS) technique at various applied voltages, it was found that the dye loading for brookite is significantly lower than that of the reference anatase film with a similar porosity and crystallite size, suggesting a lower anchoring site density for the dye on the brookite surface.[14] Moreover, the investigations of the chemical capacitance and of the charge transfer resistance (R_{ct}) show that, compared to anatase, the brookite surface is less

active for the recombination side reaction. The larger R_{ct} is shown to explain the higher V_{OC} of the brookite cells. However, the charge transport is much slower in the brookite phase due to a lower electrical conductivity.[14] This parameter has been quantified more than 1 order of magnitude lower in the brookite layers compared to the anatase one.[14] Therefore, it can be concluded that the higher V_{OC} of the present brookite cell can be attributed to the lower surface reactivity and the higher Fermi level of the brookite TiO_2 nanocubes compared to the anatase TiO_2 nanoparticles as mentioned above.

Nevertheless, the present brookite cell's efficiency (3.92%) is much lower than that (7.13%) of the anatase cell. Although both of the solar cells have a similar film thickness, the brookite film shows much lower dye loading than the anatase one as shown in Table 1. On one hand, this result is similar to the previous report that anatase TiO_2 film has a significantly higher dye loading compared to the brookite TiO_2 with the same porosity and particle size,[14] which can be ascribed to the higher density of dye anchoring sites on the anatase surface compared to brookite.[12-14] On the other hand, the present brookite nanocubes has much larger average size (~50 nm) than the nanosized anatase (~20 nm) as mentioned above, which would lead to a less surface area and lower dye loading compared to T2 film with a similar thickness, and then causing the brookite cell (B2) show the lower photocurrent and efficiency than the anatase one (T2). Moreover, it has reported that the poor conductivity of brookite could lead to the significantly lower collection efficiency in the brookite cell.[14] Although it can also slow the electron transport time and prolong the electron lifetime, the low efficiency of the brookite cell is mainly limited by the dye loading and the charge collection efficiency, and the latter limits the optimized electrode thickness and makes it not possible to compensate the lower dye loading by the use of thicker films.[14]

Our previous investigation indicated that the rice-like brookite TiO_2 particles with ~600 nm particle diameter as

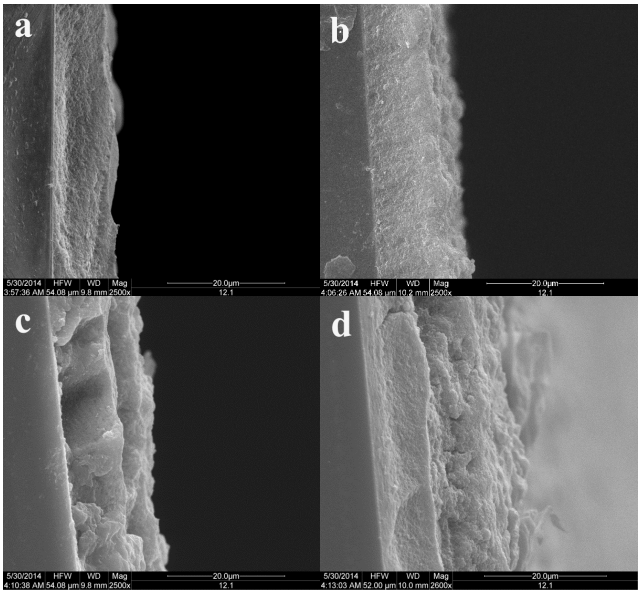

Fig. 7 Typical SEM images of the cross sections for the fabricated T2 (a), and bilayer T2B1 (b), T2B2 (c), T2B3 (d) electrodes

overlayer can enhance the V_{OC} of a nanosized anatase solar cell,[28,29] and the nanosized anatase TiO_2 film (T2 electrode) fabricated by using TPP3 paste and 2 layers of adhesive tape as spacer shows the highest efficiency.[29] Therefore, the present brookite TiO_2 nanocubes are also used as overlayer of the T2 electrode to fabricate a bilayer solar cell. Fig. 6a and 6b depict the corresponding *J-V* and dark current curves of the single anatase cell and the bilayer cells with different brookite thicknesses, and the corresponding photovoltaic parameters are listed in Table 1. Fig. 7 shows the typical SEM images of the cross sections for the T2 film and the bilayer films (T2B1, T2B2, and T2B3), which is fabricated with brookite overlayer on T2 film by using 1, 2, and 3 layers of adhesive tape as spacer, respectively. Obviously, those bilayer solar cells show much higher J_{SC} and V_{OC}, and then causing a significant increase in the conversion efficiency compared to the single anatase cell.

The addition of the brookite overlayer demonstrates distinct increase in the photovoltaic parameters of the anatase cell. T2B1 film gives an obviously increased J_{SC} (17.04 mA cm^{-2}) compared to the T2 film (15.27 mA cm^{-2}), and this increase in J_{SC} slows down with enhancing the brookite thickness (T2B2), and then drops to 16.78 mA cm^{-2} for the T2B3 film. The thicker film results in the increased dye loading (Table 1), which would be responsible for the increase in the J_{SC} when the film thickness is enhanced from 10.6 to 17.5 μm; whereas too long transport route of the injected electrons from TiO_2 nanoparticles towards FTO layer for the thicker film also results in an increased charge recombination, which is no benefit to the improvement in the cell's efficiency. Meanwhile, the addition of the brookite overlayer also enhances V_{OC} of the single anatase cell, which approaches to maximum for the T2B2 film. One possible reason for the V_{OC} enhancement might be the higher CB of brookite than the anatase as mentioned above.[21]

Generally speaking, the photovoltaic performance of the present bilayer solar cells is more dependent on J_{SC} behavior than the other parameters as shown in Table 1. Among those bilayer films tested, T2B2 has an optimal brookite film thickness, the corresponding bilayer solar cell gives a conversion efficiency up to 8.83%, with a 23.8% improvement as compared to the single anatase cell (7.13%). Typical incident

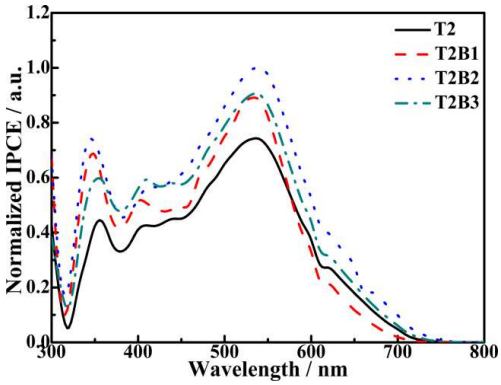

Fig. 8 Normalized monochromatic IPCE curves of the DSSCs fabricated with the single anatase film and the bilayer films

photon-to-electron conversion efficiency (IPCE) curves of the single anatase cell and the bilayer solar cells are shown in Fig. 8. Peak at ~360 nm and ~530 nm are related to the intrinsic absorption of TiO_2 and N719, respectively. The integration of IPCE curves keep the same order of the above photocurrent and conversion efficiency, and the IPCE values has a significant increase in the full spectrum after coating the brookite overlayer on T2 film. Both the anatase and the brookite nanoparticles contribute immeasurably to the light harvesting, and the light absorption is directly proportional to the film thickness to a certain extent. However, the film thickness is not the single influencing factor, which can be further validated by the following photoelectrochemical measurements.

3.3 Photoelectrochemical behavior analyses of the solar cells

To investigate the photoelectrochemical reaction kinetics during the DSSCs operations, electrochemical impedance spectra (EIS) are obtained at the open-circuit voltage of the solar cells under AM1.5 illumination. Typically, Nyquist diagram features three semicircles that in the order of increasing frequency are attributed to the Nernst diffusion within the electrolyte, the electron transfer at the TiO_2/electrolyte interface, and the redox reaction at Pt electrode.[40] In our EIS diagrams, two obvious semicircles are detected in the Nyquist plots (Fig. 9a). The semicircle attributed to the Nernst diffusion in the electrolyte is featureless due to the relatively fast diffusion of the electrolyte in the present porous films.[41] As stated above, the semicircle in high frequency region should be ascribed to the charge transfer resistance at the electrolyte/Pt electrode interface (R_1); and the semicircle in middle frequency region is related to the electron accumulation/ transport in the TiO_2 film and the charge transfer across either the TiO_2/electrolyte or the FTO/TiO_2 interfaces (R_2); R_s represents the serial resistance which is determined by the sheet resistance between the TiO_2 and the FTO layers.

According to the equivalent circuit model inserted in Fig. 9a and the corresponding fitted parameters listed in Table 2, the R_s and R_1 values of those bilayer solar cells are basically similar to the single anatase cell, implying the addition of the brookite layer on the anatase film has no obvious influence on the charge transfer resistances at the electrolyte/Pt electrode and the TiO_2/FTO interfaces. This is reasonable since both of the two kinds of solar cells have the same anatase TiO_2/FTO interfaces and the Pt electrode. Therefore, it can be concluded that the structure difference between the TiO_2/electrolyte interface plays a decisive role on their photovoltaic performance. Namely, the addition of the brookite overlayer leads to a significantly reduced R_2 values, indicating the charge transfer process at the bilayer TiO_2/electrolyte interface is more efficient than that at the single anatase TiO_2/electrolyte interface. It would be beneficial for enhancing the electron injection efficiency. Moreover, the higher CB of the brookite than anatase is also a benefit of the electron injections from the brookite layer to the anatase TiO_2 film, which could produce stronger driving force for the electron injection in the bilayer cell. As mentioned

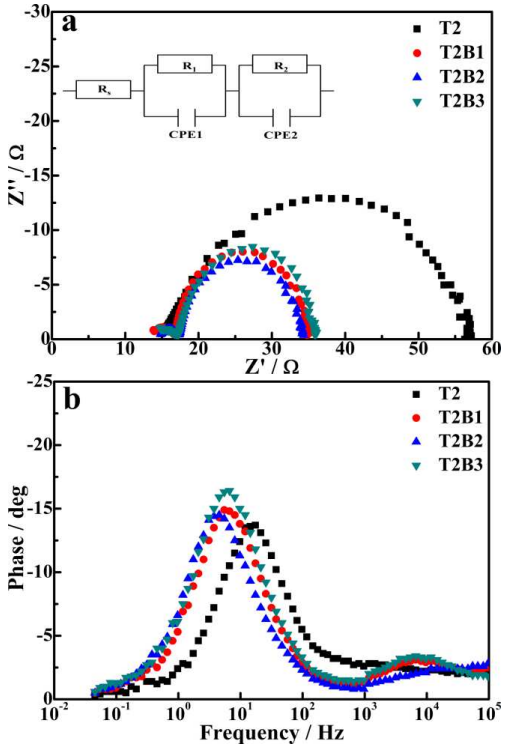

Fig. 9 Electrochemical impedance spectroscopy (EIS) of the DSSCs fabricated with the single anatase film and the bilayer films: Nyquist plots (a); Bode plots (b)

Table 2 Electrochemical parameters of the DSSCs fabricated with different electrodes

Samples	R_S Ω cm^2	R_1 Ω cm^2	R_2 Ω cm^2	f Hz	τ_n ms
T2	14.82	2.25	42.2	16.1	9.9
T2B1	14.80	2.36	19.8	6.2	25.7
T2B2	13.85	2.27	18.0	4.3	37.0
T2B3	14.81	2.33	21.9	6.1	26.1

above, a low R_2 implies the electrons can transport a longer distance with less diffusive hindrance to some extent, and thus probably leading to the reduced electron recombination and the more effective electron capture.[41] As seen from Table 2, the R_2 value for the T2B2-based cell shows the lowest one among those cells tested, only 42.7% of the value of the anatase cell without overlayer; while R_2 increased obviously when the film thickness exceed the optimized one. This is consistent with the above changes in the photocurrent and conversion efficiency.

The lifetime (τ_n) of injected electrons in the solar cell can be determined by the position of the low frequency peak in the Bode plots through the equation $\tau_n=1/(2\pi f)$, where f means the frequency of superimposed AC voltage.[40] As can be seen in Fig. 9b, the f values of devices with the brookite overlayers are much lower than that of the single anatase cell. Namely, the addition of the brookite overlayer can significantly prolong the electron lifetime (Table 2). Once again, T2B2-based cell shows the longest lifetime (37 ms) among those cells tested, enhanced

by 2.74 times compared to the anatase cell, also indicating the best photovoltaic performance. The longer electron lifetimes of those bilayer solar cells can also be ascribed to the poor conductivity of brookite compared to anatase, which means a reduced charge recombination, and then causing the enhanced V_{OC} of the bilayer cell compared to the anatase one.[14]

Open-circuit voltage decay (OCVD) curve can provide the main information on the interfacial recombination processes between the injected electrons in the TiO_2 film and electrolyte.[39-43] Under the open-circuit and dark conditions, the electron transport resistance in the TiO_2 film has no effect on the OCVD measurements because there is no current flow through the cell. The difference of cell's V_{OC} can change the electron lifetime (τ_n') due to the Fermi level shift of semiconductors. Hence, the shape of τ_n'~V_{OC} relation curve of the solar cell can qualitatively reflect the effects of the electron traps on the recombination reaction. The electron lifetime (τ_n') can be derived from the OCVD measurements according to eqn (1):

$$\tau_n' = -\frac{k_B T}{e}\left(\frac{dV_{OC}}{dt}\right)^{-1} \qquad (1)$$

where k_B is the Boltzmann constant, T is the temperature, e is the electron charge.

Once the light was shut off, the V_{OC} of the single anatase cell decays near to 0 only after 20s decay time as shown in Fig. 10a, while T2B1, T2B2, and T2B3 bilayer solar cells still maintains ~0.1, 0.3, and 0.05 V even after 60 s, respectively. It implies the bilayer solar cells have less charge recombination and longer electron lifetime than the single anatase one.

As can be seen from the τ_n'-V_{OC} relation curves shown in Fig. 10b, the electron lifetimes (τ_n') show an exponential dependence at the V_{OC}. According to Zaban's suggestion,[44] a typical τ_n'~V_{OC} curve can be divided into three parts in which the lifetime is dominated by different factors: a constant lifetime at high voltage related to free electrons, an exponential dependence at medium potential due to the internal trapping and detrapping, and an inverted parabola at low voltage corresponding to the reciprocal of the density of levels of acceptor electrolyte species. The linear dependence of electron lifetime on V_{OC} turned into a curved one because the charge transfer process is mainly governed by the distribution of surface state traps.[39,44] The electron lifetime increases significantly at medium and low voltage regions after the addition of the brookite overlayer.

As mentioned above, the brookite nanocubes has much larger size than the anatase TiO_2 nanoparticles of the TPP3 paste, which would lead to less grain boundaries in the bilayer film as compared to the single anatase one, and then causing the decrease of the surface traps. In other words, the bilayer solar cells should have more efficient interfacial charge transfer process than the single anatase one, which further results in the less charge recombination due to the surface traps, and then the prolonged electron lifetime. Meanwhile, the present brookite particles with a higher CB coating on anatase film can also block the back flow of the injected electrons, which can be inferred from the higher remaining voltage in the OCVD curves (Fig. 10a), and then decreases the charge recombination and the dark current. As shown in Fig. 8b, the single anatase cell shows much higher dark current than those bilayer ones, certifying the electrons' backflow (recombination) could be reduced by the

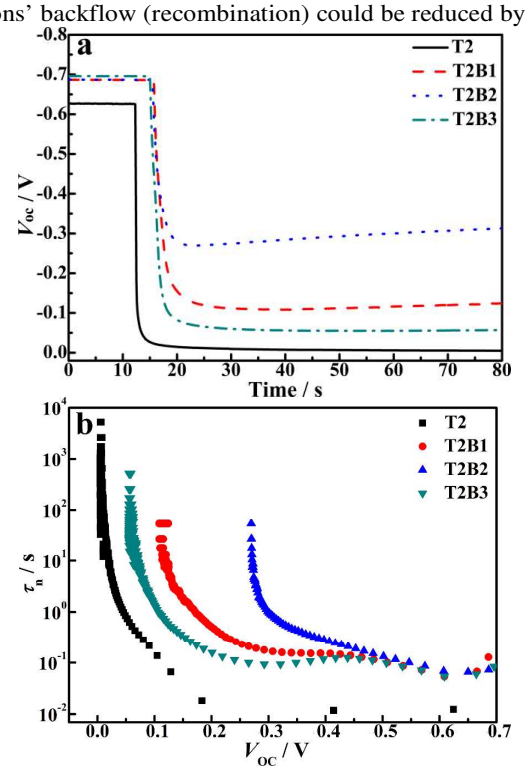

Fig. 10 Open-circuit voltage decay (OCVD) curves of the DSSCs fabricated with the single anatase film and the bilayer films.

brookite overlayer. Moreover, it was reported that the dark current can affect V_{OC} strongly, and a low dark current usually benefit for obtaining a high voltage.[45] This is consistent with our observation that all bilayer solar cells bring out higher V_{OC} compared to the single anatase one.

On the basses of the above results and discussion, the present brookite TiO_2 nanocubes with small size and high phase purity can be used as overlayer of the nanosized anatase TiO_2 film. The obviously improved photovoltaic performance of the bilayer solar cells can be mainly ascribed to the following reasons. 1) Although the brookite TiO_2 has much lower dye loading than the anatase TiO_2 due to its less dye anchoring sites, the addition of brookite overlayer still can cooperates with the anatase film to load more dye molecules, which leads to the bilayer solar cells showing significantly enhanced J_{SC} compared to the single anatase one; 2) Brookite overlayer can also reduce the grain boundaries in the bilayer film/electrolyte interfaces, it means that the bilayer cells would have significant decreases in the surface traps and the charge recombination, which results in longer electron lifetime than the single anatase cell. 3) The higher CB level of the brookite than anatase TiO_2 is also a benefit of the electron injections from the brookite overlayer to the anatase film, which could produce a stronger driving force for the electron injection in the bilayer cells, and also retard the charge recombination (electrons flowing back to the electrolyte) and the dark current, and then causing a high

voltage. As a result, the bilayer TiO_2 solar cell with the optimized brookite thickness gives a conversion efficiency of 8.83%, with a 23.8% improvement as compared to the single anatase one (7.13%). Although the low dye loading and the charge collection efficiency leads to the not very satisfactory efficiency of the single brookite cells, the present brookite nanocubes as overlayer of the anatase film could generate some additional advantages, such as less surface state traps, longer electron lifetime, reduced charge recombination and dark current. All these would lead to a more efficient electron injection, higher voltage and photocurrent, and then causing the improved photovoltaic perforce of the bilayer solar cell.

4 Conclusions

In summary, brookite TiO_2 quasi nanocubes with high phase purity were synthesized through a simple hydrothermal method. By using as photoanode material, the brookite TiO_2 nanocubes film-based solar cell shows a higher open-circuit voltage but lower conversion efficiency than the nanosized anatase TiO_2 film-based one with a similar film thickness; while using the brookite nanocubes as overlayer of the anatase TiO_2 film, the fabricated bilayer TiO_2 film-based solar cells exhibit significant enhancement in both the open-circuit voltage and short-circuit current density, and then causing a better conversion efficiency. After optimizing the thicknesses of overlayer, the corresponding bilayer TiO_2 film-based solar cell gives an efficiency of 8.83%, with a 23.8% improvement as compared to the single anatase one (7.13%). The brookite nanocubes as overlayer of the anatase film could generate some additional advantages such as lower charge transfer resistance, less surface state traps, longer electron lifetime, reduced charge recombination and dark current. All these would lead to higher voltage and photocurrent, and then causing the improved photovoltaic performance of the bilayer solar cell. The present results demonstrate that the simple fabrication method of the brookite nanocubes and its application as overlayer of anatase electrode are promising, which offers a strategy for the development of the low-cost and high efficiency DSSCs through tuning the photoanode's component and structure.

Acknowledgements

This work was supported by the National Natural Science Foundation of China (21271146, 20973128, and 20871096), the Funds for Creative Research Groups of Hubei Province (2014CFA007), and Fundamental Research Funds for the Central Universities (2042014kf0228), China

References

1 A. L. Linsebigler, G. Lu and J. T. Yates, *Chem. Rev.,* 1995, **95**, 735.
2 J. Mao, L .Q. Ye, K. Li, X. H. Zhang, T. Y. Peng and L. Zan, *Appl. Catal. B,* 2014, **144**, 855.
3 J. Burschka, N. Pellet, S. J. Moon, R. Humphry-Baker, P. Gao, M. K. Nazeeruddin and M. Grätzel, *Nature*, 2013, **499**, 316.
4 D. Liu and T. L. Kelly, *Nature Photon.,* 2014, **8**, 133.
5 S. D. Mo and W. Y. Ching, *Phys. Rev. B,* 1995, **51**, 13023.
6 M. M. Rodriguez, X. H. Peng, L. J. Liu, Y. Li and J. M. Andino, *J. Phys. Chem. C,* 2012, **116**, 19755.
7 B. Ohtani, J. Handa, S. Nishimoto and T. Kagiya, *Chem. Phys. Lett.,* 1985, **120**, 292.
8 Q.F. Zhang, C. S. Dandeneau, X. Y. Zhou and G. Z. Cao, *Adv. Mater.*, 2009, **21**, 4087.
9 L. J. Zhang, V. M. Menendez-Flores, N. Murakama and T. Ohno, *Appl. Surf. Sci.*, 2012, **258**, 5803.
10 K. J. Jiang, T. Kitamura, H. Yin, S. Ito and S. Yanagida, *Chem. Lett.,* 2002, **31**(9), 872.
11 E. Lancelle-Beltran, P. Prené, C. Boscher, P. Belleville, P. Buvat, S. Lambert,F. Guillet, C. Marcel and C. Sanchez, *Eur. J. Inorg. Chem.*, 2008, **6,** 903.
12 C. Magne, S. Cassaignon, G. Lancel and T. Pauporté, *ChemPhysChem,* 2011, 12, 2461.
13 C. Magne, F. Dufour, F. Labat, G. Lancel, O. Durupthy, S. Cassaignon and T. Pauporté, *J. Photochem. Photobiol. Chem.,* 2012, **232**, 22.
14 Y. Kusumawati, M. Hosni, M. A. Martoprawiro, S. Cassaignon and T. Pauporte, *J. Phys. Chem. C,* 2014, **118**, 23459.
15 M. Koelsch, S. Cassaignon, T. T. Minh, J. F. Guillemoles and J. P. Jolivet, *Thin Solid Films,* 2004, **451/452**, 86.
16 T. A. Kandiel, L. Robben, A. Alkaim and D. Bahnemann, *Photoch. Photobio. Sci.* 2013, **12**, 602.
17 Y. L. Liao, W. X. Que, Q. Y. Jia, Y. C. He, J. Zhang and P. Zhong, *J. Mater. Chem.,* 2012, **22**, 7937.
18 J. G. Li, T. Iahigaki and X. D. Sun, *J. Phys. Chem. C*, 2007, **111**, 4969.
19 T. Mitsuhashi and M. Watanabe, *Mineral. J.*, 1978, **9**, 236.
20 P. Arnal, R. J. P. Corriu, D. Leclercq, P. H. Mutin and A. Vioux, *J. Mater. Chem.*, 1996, **6**, 1925.
21 W. B. Hu, L. P. Li, G. S. Li, C. L. Tang and L. Sun, *Cryst. Growth Des.,* 2009, **9**, 3676.
22 M. Koelsch, S. Cassaignon, J. F. Guillemoles and J. P. Jolivet, *Thin Solid Films*, 2002, **403**, 312.
23 R. Zallen and M. P. Moret, *Solid State Commun.*, 2006, **137**, 154.
24 M. Grätzel and F.P. Rotzinger, *Chem. Phys. Lett.*, 2001, **118**, 474.
25 S. Ardizzone, C. L. Bianchi, G. Cappelletti, S. Gialanella, C. Pirola and V. Ragaina, *J. Phys. Chem. C*, 2007, **111**, 13222.
26 H. Kominami, J. Kato, S. Murakami, Y. Ishii, M. Kohno, K. Yabutani, T. Yamamoto, Y. Kera, M. Inoue, T. Inui and B. Ohtani, *Catal. Today,* 2003, **84**, 181.
27 H. F. Lin, L. P. Li, M. L. Zhao, X. S. Huang, X. M. Chen, G. S. Li and R. C. Yu, *J. Am. Chem. Soc.,* 2012, **134**, 8328.
28 K. Li, J. L. Xu, W. Y. Shi, Y. B. Wang and T. Y. Peng, *J. Mater. Chem. A,* 2014, **2**, 1886.
29 J. L. Xu, K. Li, W. Y. Shi, R. J. Li and T. Y. Peng, *J. Power Sources,* 2014, **260**, 233.
30 K. Fan, T. Y. Peng, J. N. Chen, X. H. Zhang and R. J. Li, *J. Power Sources*, 2013, **222**, 38.
31 J. Huberty and H. F. Xu, *J. Solid State Chem.*, 2008, **181**, 508.
32 S. Bakardjieva, V. Stengl, L. Szatmary, J. Subrt, J. Lukac, N. Murafa, D. Niznansky, K. Cizek, J. Jirkovsky and N. Petrova, *J. Mater. Chem.*, 2006, **16**, 1709.
33 C. Perego, Y. H. Wang, O. Durupthy, S. Cassaignon, R. Revel and J. P. Jolivet, *ACS Appl. Mater. Interfaces,* 2012, **4**, 752.
34 H. Kominami, M. Kohno and M. Kera, *J. Mater. Chem.,* 2000, **10**, 1151.
35 G. A. Tompsett, G. A. Bowmaker, R. P. Cooney, J. B. Metson, K. A. Rodgers and J. M. Seakins, *J. Raman Spectrosc.,* 1995, **26**, 57.
36 Y. H. Zhang, C. K. Chan, J. F. Porter and W. Guo, *J. Mater. Res.,* 1998, **13**, 2602.
37 W. G. Su, J. Zhang, Z. C. Feng, T. Chen, P. L. Ying, C. Li, *J. Phys. Chem. C,* 2008, **112**, 7710.
38 T. Nagase, T. Ebina, T. Iwasaki, H. Hayashi, Y. Onodera and M. Chatterjee, *Chem. Lett.,* 1999, 911.
39 K. Fan, W. Zhang, T. Y. Peng, J. N. Chen and F. Yang, *J. Phys. Chem. C,* 2011, **115**, 17213.
40 D. Zhao, T. Y. Peng, L. L. Lu, P. Cai, P. Jiang and Z. Q. Bian, *J. Phys. Chem. C,* 2008, **112**, 8486.
41 Y. Z. Zheng, X. Tao, L. X. Wang, H. Xu, Q. Hou, W. L. Zhou and J. F. Chen, *Chem. Mater.,* 2009, **22**, 928.
42 T. Y. Peng, K. Fan, D. Zhao and J. N. Chen, *J. Phys. Chem. C,* 2010, **114**, 22346.
43 R. Kern, R. Sastrawan, J. Ferber, R. Stangl and J. Luther, *Electrochim. Acta,* 2002, **47**, 4213.

44 J. Bisquert, A. Zaban, M. Greenshtein and I. Mora-Sero, *J. Am. Chem. Soc.,* 2004, **126**, 13550.
45 Q. Wang, J. E. Moser and M. Grätzel, *J. Phys. Chem. B,* 2005, **109**, 14945.

Table of Contents Graphic

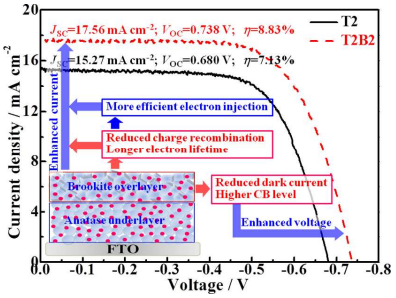

Brookite TiO_2 quasi nanocubes were synthesized and used as overlayer to fabricate bilayer TiO_2 film-based DSSCs with enhanced efficiency.